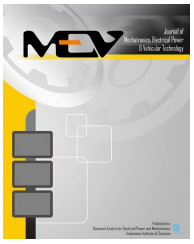

Journal of Mechatronics, Electrical Power, and Vehicular Technology 16 (2025) 95-105

Journal of Mechatronics, Electrical Power, and Vehicular Technology

e-ISSN: 2088-6985
p-ISSN: 2087-3379

mev.brin.go.id

Optimizing bioethanol from sago dregs for Honai burner stoves: A case study in Papua

Johni Jonatan Numberi [a, *], Tiper Korneles Muwarberto Uniplaita [b], Agri Suwandi [c], Januar Parlaungan Siregar [d], Arifia Ekayuliana [e], Joni Joni [a], Pither Palamba [a], Marthen Liga [b]

[a] *Department of Mechanical Engineering, Universitas Cenderawasih*
Jl. Kamp Wolker, Yabansai, Jayapura, 99351, Indonesia

[b] *Department of Electrical Engineering, Universitas Cenderawasih*
Jl. Kamp Wolker, Yabansai, Jayapura, 99351, Indonesia

[c] *Department of Mechanical Engineering, Universitas Pancasila*
Jl. Lenteng Agung Raya No.56, RT.1/RW.3, Srengseng Sawah, Jagakarsa, South Jakarta, 12630, Indonesia

[d] *Department of Mechanical Engineering, Universiti Malaysia Pahang*
Al-Sultan Abdullah, Pekan, Pahang, 26600, Malaysia

[e] *Department of Mechanical Engineering, Politeknik Negeri Jakarta*
Jl. Prof. DR. G.A. Siwabessy, Kukusan, Beji, Depok, West Java, 16425, Indonesia

Abstract

Indonesia harbors considerable prospects for bioethanol fuel generation. Underscoring the imperative for establishing optimal fuel concentrations and appropriate burners to facilitate sustainable energy alternatives; this study endeavored to identify the optimal bioethanol concentration sourced from sago waste for application in Honai burners, evaluating the resultant flame output for domestic energy in Papuan custom houses. This analysis adopted an integration of pre-experimental frameworks along with experimental ones. In the early trial stage, concentrations of bioethanol were thoroughly examined concerning low heat value (LHV), specific gravity, viscosity, gas chromatography, and Fourier transform infrared (FTIR) analysis to identify the best fuel characteristics. Following this, the experimental phase assessed flame characteristics, encompassing temperature, fuel mass flow rate, and emissions from combustion gases within the Honai burner. Pre-experimental findings suggest that an 80 % bioethanol concentration is ideal for the Honai burner, displaying a viscosity of 1.03 cP, a density of 0.82 g·L^{-1}, a gas chromatography content of 61.04 %, an LHV of 16.166 MJ/kg, and a heat release rate of 140 kW·m^{-2}. The experimental phase indicates that a 14-hole burner oriented at a 45° angle yields optimal performance, achieving stable flame temperatures between 480 °C and 750 °C with a fuel flow rate of 60 mL·min^{-1}. Analysis of combustion gases indicates minimal emissions, with carbon monoxide (CO) registering at 0.01 %, carbon dioxide (CO_2) at 0.2 %, and hydrocarbons (HC) at 27 ppm. In summary, this study offers a feasible approach to addressing energy challenges, meeting demand, enhancing accessibility, ensuring availability, and promoting regional energy autonomy for Papuan households in remote locales through the utilization of bioethanol derived from sago dregs in Honai burner cooking devices.

Keywords: sago dregs; bioethanol; flame temperature; heat release; Honai burner; Papuan households.

* Corresponding Author. j_numberi@yahoo.com (J. J. Numberi)

https://doi.org/10.55981/j.mev.2025.1053

Received 19 February 2025; revised 24 June 2025; accepted 30 June 2025; available online 30 July 2025; published 31 July 2025

How to Cite: J. J. Numberi *et.al.*, "Optimizing bioethanol from sago dregs for Honai burner stoves: A case study in Papua," *Journal of Mechatronics, Electrical Power, and Vehicular Technology*, vol. 16, no. 1, pp. 95-105, July, 2025.

I. Introduction

Indonesia is experiencing an increasing demand for bioethanol, which is predicted to rise by 10 to 15 % from 2016 to 2025, leading to a total requirement of 30,833,000 L/month [1]. By 2025, biofuels, including bioethanol, are projected to replace 1.48 billion liters of gasoline, accounting for 5 % of hydrocarbon consumption in the country [2]. This transition is in line with the objective of the government to gradually adopt renewable energy system by 2050 [3]. Meanwhile, bioethanol is manufactured from local plants, such as cassava [4][5][6], avocado [7][8], corncobs [9], Napier grass [10], and sago [11][12][13][14]. Sago is highly valuable for carbohydrates, and cellulose production is essential for manufacturing bioethanol [15]. Each stem produces 200 to 500 kg of moist starch annually, equivalent to 25 to 30 tons per hectare, which is a significant energy source [16]. An estimated 51.3 % of sago fields globally, with the potential for bioethanol fuel production, are located in Indonesia [17].

Global statistics reveal that approximately 6.5 million hectares are allocated to sago cultivation [18], with Indonesia accounting for a substantial 85 %, equating to around 5.5 million hectares. These regions are classified into natural sago forests and cultivated plantations, encompassing 5,294,538 hectares and 205,462 hectares, respectively. Approximately 94.5 % of Indonesia's sago resources, equating to around 5.2 million hectares, are concentrated in Papua [19]. This highlights Papua's considerable capacity for advancing alternative and renewable energy resources [11].

Bioethanol (C_2H_5OH), an alternative fuel, is more environmentally friendly compared to kerosene, produces fewer carbon emissions, and is derived from renewable resources [11]. However, there is a need to carry out extensive research and awareness, specifically on the use of sago dregs waste as a source of bioethanol production. An analysis conducted using photo-scanning electron microscopic energy-dispersive X-ray (EDX) testing shows the structure of the hydrocarbon components in Papuan sago dregs comprises significant carbon content of 70.91 % and 76.49 % by dry and wet weights, respectively. Dregs also contain oxygen, constituting approximately 28.95 % and 23.45 % by dry and wet weights, including 0.14 % and 0.06 % silicone by dry and wet weights, respectively. In addition, it comprises 82.4 %, 10.4 %, 3.64 %, 1.85 %, 1.70 %, and 0.01 % of carbohydrates, water, ash, proteins, coarse fiber, and fat [15].

The fundamental combustion characteristics of bioethanol is paramount for optimizing burner performance and ensuring safe, efficient domestic energy solutions [19]. Key parameters include the air-fuel ratio (AFR), which defines the proportion of air to fuel necessary for complete combustion, and the stoichiometry of hydrocarbon fuels [20]. Flame characteristics, such as the behavior of diffusion and laminar flames, are also critical, as their energy content influences reactant diffusion and overall stability [21]. Furthermore, burner geometry, including the size of jet holes and nozzle design, significantly impacts flame stability and overall burner performance [22], making its precise consideration vital for the Honai burner application.

To date, no studies have evaluated sago-dregs bioethanol in the context of Honai burner stoves, a key domestic energy technology for isolated Papuan communities. This gap prevents informed recommendations on optimal bioethanol blends and burner geometries for stable, efficient combustion. The present work therefore aims to (1) identify the optimal concentration of sago-dregs bioethanol based on fuel properties, and (2) assess flame characteristics, combustion efficiency, and emissions in a 14-hole, 45°–tilted Honai burner. By linking fuel chemistry to burner performance, this study provides actionable insights for sustainable household energy solutions in Papua.

II. Materials and Methods

The method comprised two phases, namely pre-experimental and experimental. The characteristics of bioethanol fuel derived from sago dregs were determined in the pre-experimental phase. The experimental phase includes setting up combustion equipment to collect data on flame temperature distribution, hot gas, and smoke behavior, pressure distribution in the tube and burner, exhaust gas production during the combustion, flame phenomena, and height.

A. Pre-experimental characterization

Figure 1 shows the method of producing fuel from sago dregs, namely milling, hydrolysis, fermentation, and distillation. The distillation method produces the fuel, which is subsequently pumped into Honai burner for usage.

Bioethanol produced during the pre-experimental method has varying concentrations, ranging from 80 % volume. These concentrations produced sufficient flame output than values above 60 %. Bioethanol is transferred into the conduit, connected to a flowmeter-controlled hose, for further experimentation. The pre-experiment aims to determine the optimal bioethanol concentration with sufficient flame performance when used in Honai burner. Based on the measurement result,

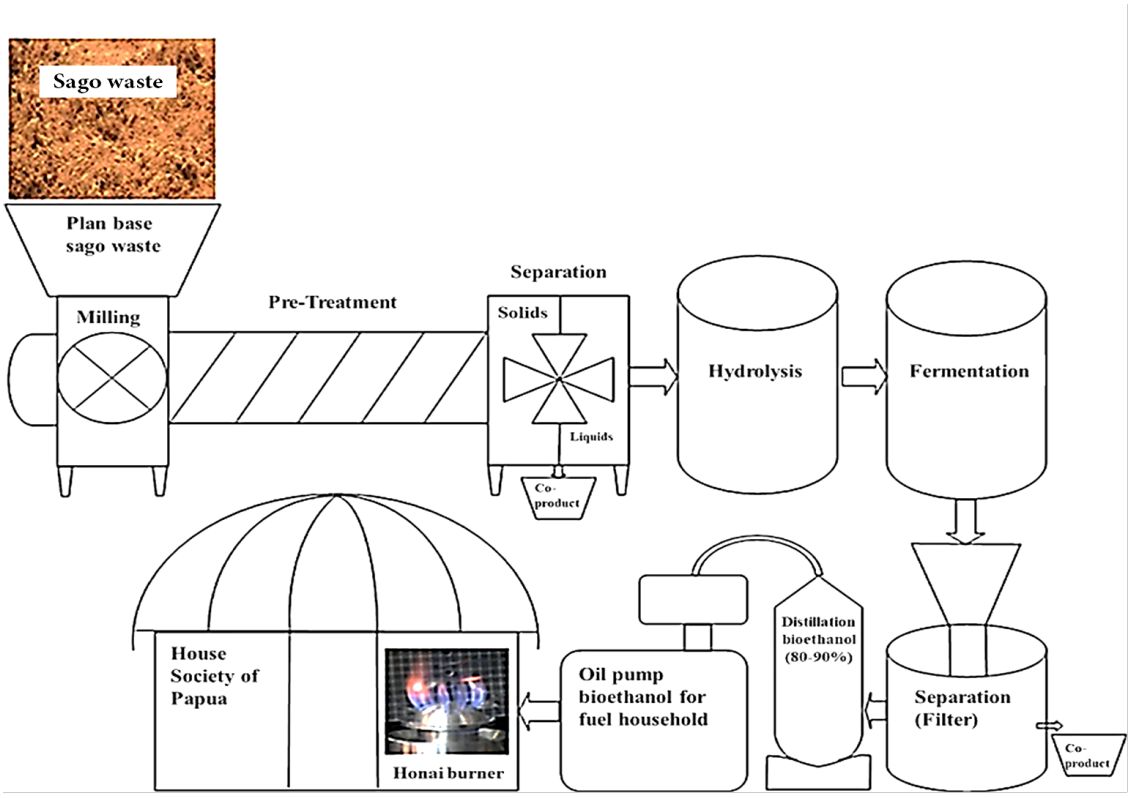

Figure 1. Production method of sago dregs bioethanol.

the most optimal concentration for fueling Honai burner was determined.

The pre-experimental method comprised five sequential steps as shown in Figure 2. Sago collection process shown in Figure 2(a). After the collection, the dreg was processed, and a smooth output was obtained, as shown in Figure 2(b). The substance was further subjected to distillation and fermentation, as shown in Figure 2(c) and Figure 2(d), respectively. The output of the entire pre-experimental method was bioethanol, which was used as fuel in the burner, as shown in Figure 2(e). In addition, five tests were conducted to ascertain the quality of bioethanol, such as low heating value (LHV), specific gravity, viscosity, gas chromatography, and Fourier transform infrared (FITR).

The first quality assessment included determining LHV according to the ASTM D4809-09a, a standard method for precisely measuring the heat of liquid

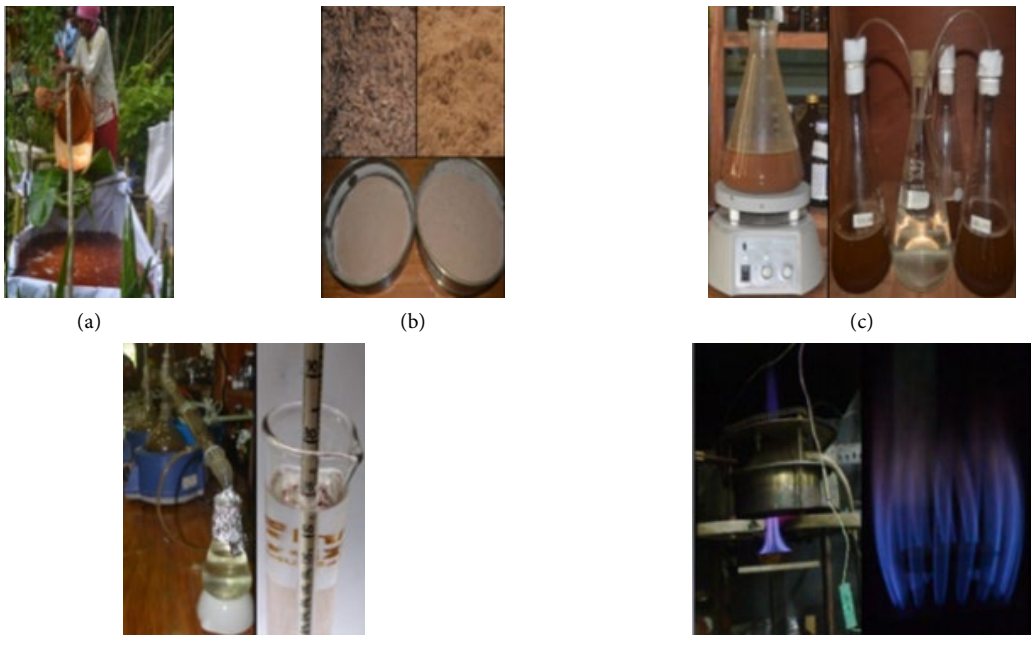

(a) (b) (c) (d) (e)

Figure 2. Pre-experimental set-up for the production of bioethanol from sago dregs: (a) Sago collection process; (b) Sago dregs; (c) Fermentation Process; (d) Distillation process; (e) Honai Burner.

hydrocarbons (HC) using a bomb calorimeter [23]. Four specific apparatuses were used in the test, namely a bomb, calorimeter, jacket, and thermometer. The method was applied to calculate temperature changes before, during, and after combustion. In the pre-experimental method, bioethanol samples with varied concentrations were used. Each sample, weighing 0.01 mg, was placed in the bomb and ignited while measuring temperature of the surroundings. In addition, the varying temperature was further used to calculate LHV of the sample.

In the second stage, the specific gravity of bioethanol was measured using a pycnometer, adhering to the ASTM D1298 method. This method entailed filling a pycnometer of known weight with bioethanol sample. Subsequently, the pycnometer was immersed in a water bath at 15 °C to stabilize temperature. The weight comparison of the pycnometer before and after the pycnometer was filled with the sample at 15 °C was used to calculate the specific gravity.

Viscosity was measured in the third stage based on the ASTM D445-23 standard. This test included the use of a calibrated glass capillary as a viscometer. Viscosity value was determined by measuring the time it takes for a volume of bioethanol sample to flow under gravity through the glass [24].

In the fourth stage, the gas chromatography was measured using Shimadzu GC-2010. The steps included injecting bioethanol sample into the GC-2010 instrument, which then analyzed and generated the measurement results.

FTIR test was conducted using the SupelCowax-10 at temperature of 50 °C in the fifth stage. A 50 µL sample of bioethanol was put on the plate in the SupelCowax-10 equipment. The test output showed bioethanol content based on the response to the infrared spectrum.

B. Combustion experiments

In the second phase, experiments were conducted to measure the performance of flame produced by the burner. This included measuring the laminar jet flame diffusion of bioethanol through direct visualization and determining flame temperature using a thermocouple [24]. Combustion byproduct gases were measured using a flue gas analyzer, while burner pressure and fuel flow rate were determined using pressure and flow meters, respectively [25]. Another experiment was conducted in a combustion chamber equipped with 14 holes and varying concentrations of bioethanol fuel.

The experimental setup, shown in Figure 3, mainly used National Instrument equipment such as the NI 9213 and NI cDaq-9172 to measure temperature of flame. These instruments are connected to the computer, facilitating the measurement data recording using LabView software. Furthermore, a DSLR Camera was positioned in front of the burner to capture the entire combustion. The data from the experiment were recorded using LabView software, with Table 1 showing the eleven steps.

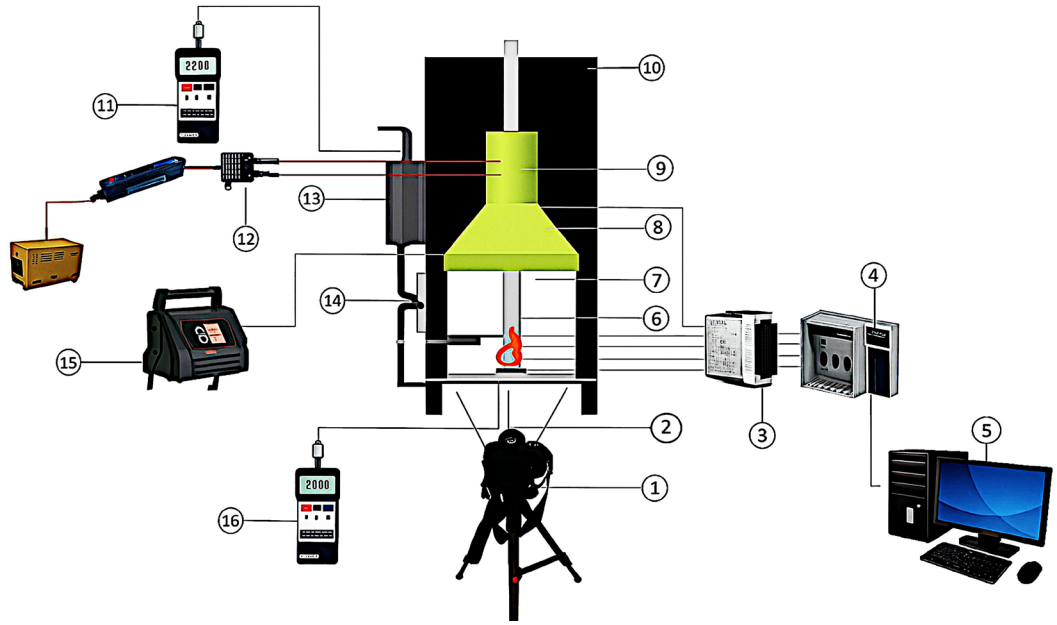

Annotation:
1. Camera
2. Honai burner
3. NI 9213
4. NI eDaq-9172
5. Computer equipment
6. Ruler
7. Combustion room, close burning
8. Ducting
9. Orifices
10. Stove tools setup
11. Pressure meter for tubes
12. Pressure sensor
13. Tube
14. Flowmeter
15. Gas analyzer
16. Pressure meter for burner

Figure 3. Experimental set-up.

Table 1.
Steps of the experiment.

No	Steps of the experiment	Equipment used at the experiment
1	Prepare the apparatus required to conduct the test	Stove, burner, bioethanol tube, flow meter, thermocouple, flue gas analyzer, pressure meter, pressure transducer, pressure drop sensor, camera, tripod, and AC-DC inverter
2	Setup a computer with the software LabView and Lutron Pressure Transducer	Lutron pressure transducer
3	Ensure bioethanol concentration is appropriate	Alcohol meter
4	Prepare 500 ml bioethanol fuel with the selected concentration	Measuring cup
5	Fill bioethanol containers	
6	Adjust the fuel consumption rate	Flow meter
7	Combustion occurred for ten minutes without waiting for the fuel to run out	
8	Flame temperature and several other temperatures at other sites were recorded	LabView software
9	The pressure in the conduit and burner was recorded	LabView software
10	Record the exhaust gas output and pressure decrease	Camera
11	The fuel rate closed after 10 minutes	Flowrate
12	Observe the residual burning fuel until the fire is extinguished and the recording stopped	

The burner was ignited and allowed to stabilize for two minutes (pre-heating), followed by an eight-minute combustion period during which all measurements were continuously logged . Upon completion, the fuel inlet was closed and the residual flame was observed until extinction.

III. Results and Discussions

A. Sago-dregs bioethanol-based properties

The results obtained proved the feasibility of bioethanol as a fuel source, particularly focusing on the qualities of flame powered by 80 % bioethanol derived from sago dregs waste, as shown in Figures 4 to Figure 8. Figure 4(a) shows LHV, the calorific value measured using the ASTM D4809-09a method. In addition, LHV value increases with higher concentrations of bioethanol, a pattern observed in similar research using bioethanol manufactured from sweet sorghum [26].

A pycnometer is a measuring device used to determine the specific gravity of bioethanol. The results of these measurements are shown in Figure 4(b), providing insights into the varying specific gravity of bioethanol solutions. As the concentration of bioethanol increases, the specific gravity of the solution decreases and remains lower than water. This trend is in line with the results from preliminary research on the production of bioethanol from agricultural waste [27]. Information regarding viscosity of bioethanol was obtained using a kinematic viscosity meter with bioethanol concentration shown in Figure 4(c). The graph indicates that viscosity decreases as the concentration of bioethanol increases. This is attributed to the fact that viscosity of ethanol solution is lower than viscosity of water, and the higher the concentration of bioethanol in the solution, the greater the content [28].

The GC-2010 gas chromatography test kit was used to determine bioethanol content, and Figure 5 shows the data collected from these measurements. The gas chromatography test confirmed the presence of ethanol in bioethanol used as fuel. The conclusion was based on the analysis of graphs and tables that showed the results of bioethanol test, conducted at 80 % concentration.

FTIR data collection served as a valuable tool for discerning organic and inorganic substances. The collection was used to make educated guesses about the proportions of mixtures containing sago dregs and bioethanol. Figure 6 shows the data obtained from the measurements, focusing on bioethanol with an 80 % concentration. Significant infrared absorption was observed in bioethanol spectrum due to O-H or alcohol stretching at 3339.07 cm^{-1}, designated as the absorption area. Meanwhile, the absorption waves at 2949.08 cm-1 signified C-H stretching groups or alkanes. Absorption at 1647.33 cm^{-1} and 1015.06 cm^{-1} showed the presence of a C = C or alkene and C = C + OH or ether bending groups, respectively. These two types of absorption show the presence of a carbon-carbon double bond.

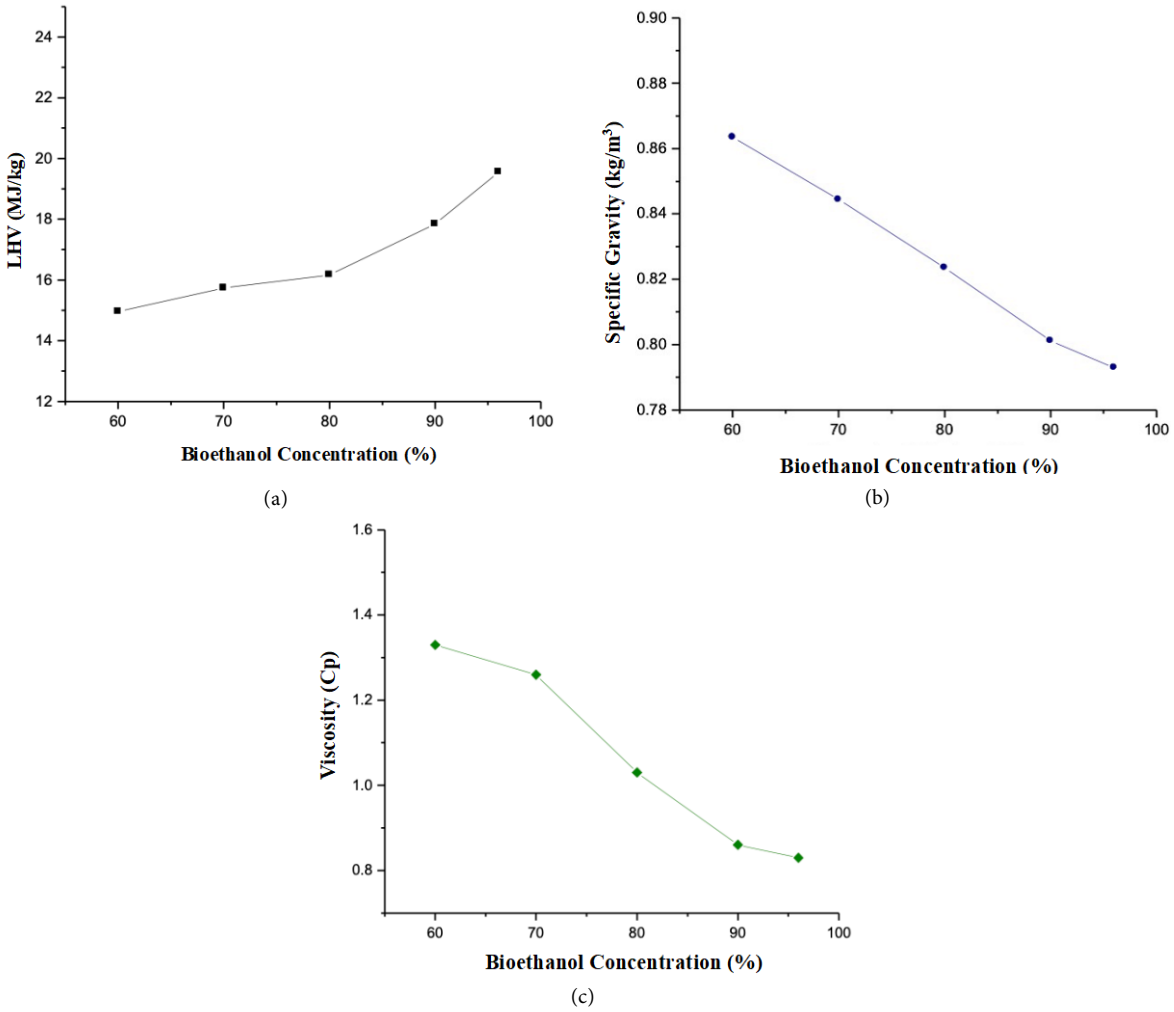

Figure 4. (a) Low Heating Value (LHV); (b) Specific gravity of bioethanol; (c) Viscosity of bioethanol.

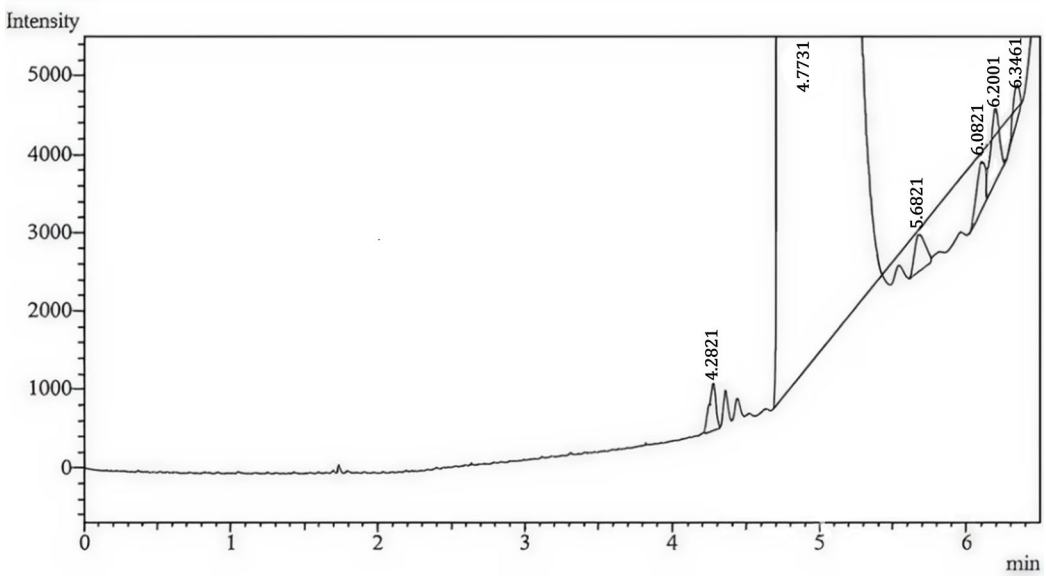

Figure 5. Gas chromatography results of 80 % concentration bioethanol test.

B. Flame characteristics

Figure 7 elucidates the combustion characteristics discerned during stable incineration utilizing 80 % v/v sago dregs-derived bioethanol. The flame displayed a distinctly delineated azure core (~10 mm), an elongated incandescent plume (~90 mm), and a terminal yellow region (~40 mm), all suggestive of proficient oxidation [29]. These attributes are emblematic of a laminar diffusion flame. Suntana *et al.* [2], along with Dhiputra *et al.* [15], have illustrated that devices for ethanol combustion demonstrate a flame form similar to this, with a steady blue core and low oscillation, which points to effective combustion. The well-

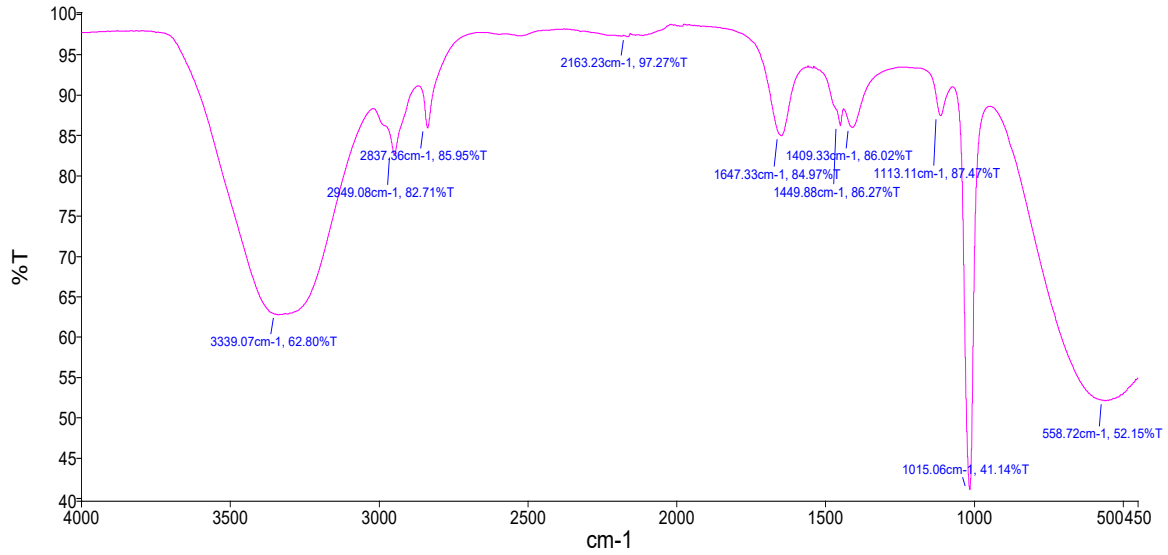

Figure 6. FTIR results of 80 % concentration bioethanol test.

articulated flame configuration observed in this investigation further substantiates that sago dregs bioethanol facilitates consistent and pristine combustion.

The performance assessment of the Honai burner fueled with 80 % v/v bioethanol involved an in-depth analysis of jet flame temperatures at a 45° inclination, as illustrated in Figure 7. Six thermocouples were strategically positioned within the combustion chamber to capture temperature readings at designated locations (points 1 through 4), as well as to monitor the thermal profiles of the resulting flue gases and smoke. The experimental setup utilized a 14-nozzle burner inclined at 45°, operating under a consistent air-to-fuel mass flow ratio of 20 mL·min^{-1}. The procedure initiated with a thermal conditioning stage enduring roughly 2 minutes, during which combustion temperatures attained values ranging from 90 °C to 100 °C.

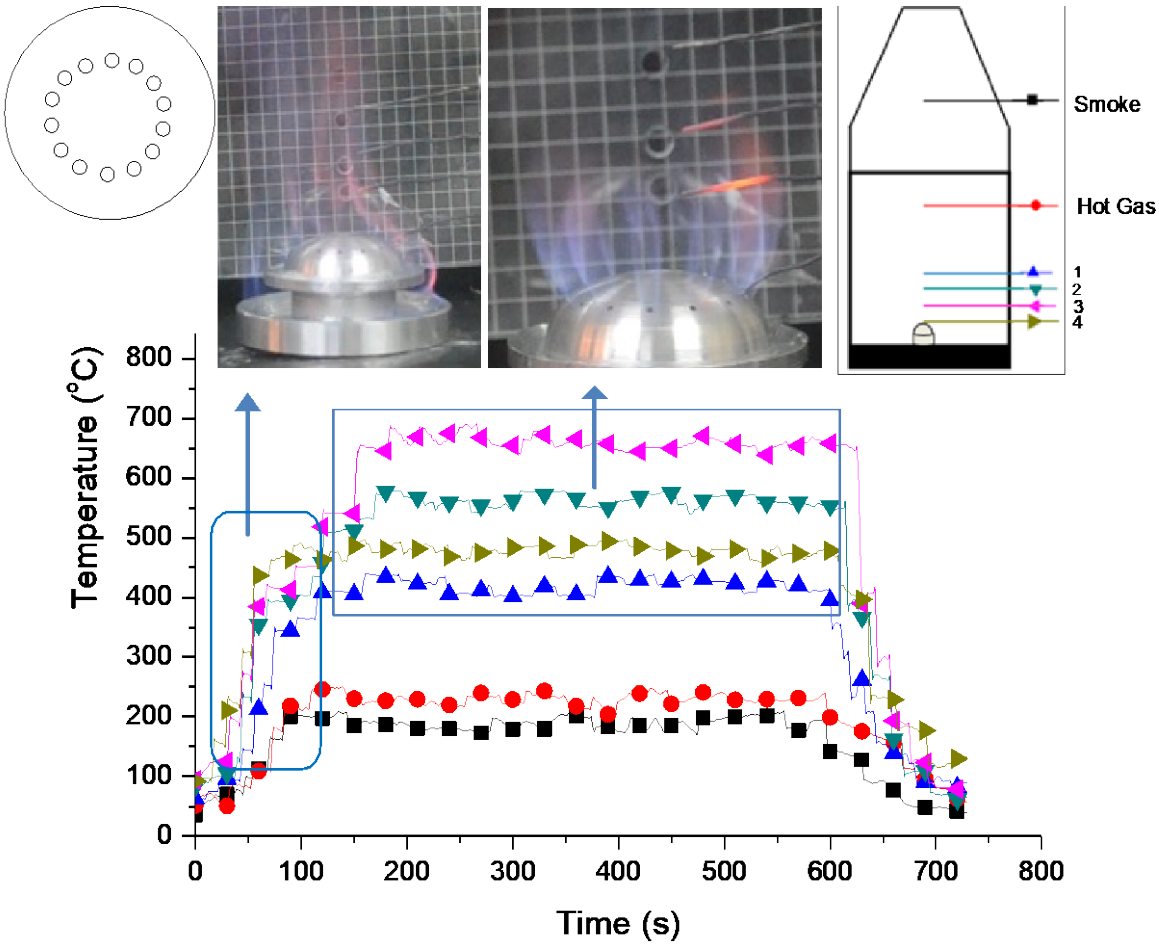

Figure 7. Temperature distribution on Honai Burner for 14-hole degrees 30.

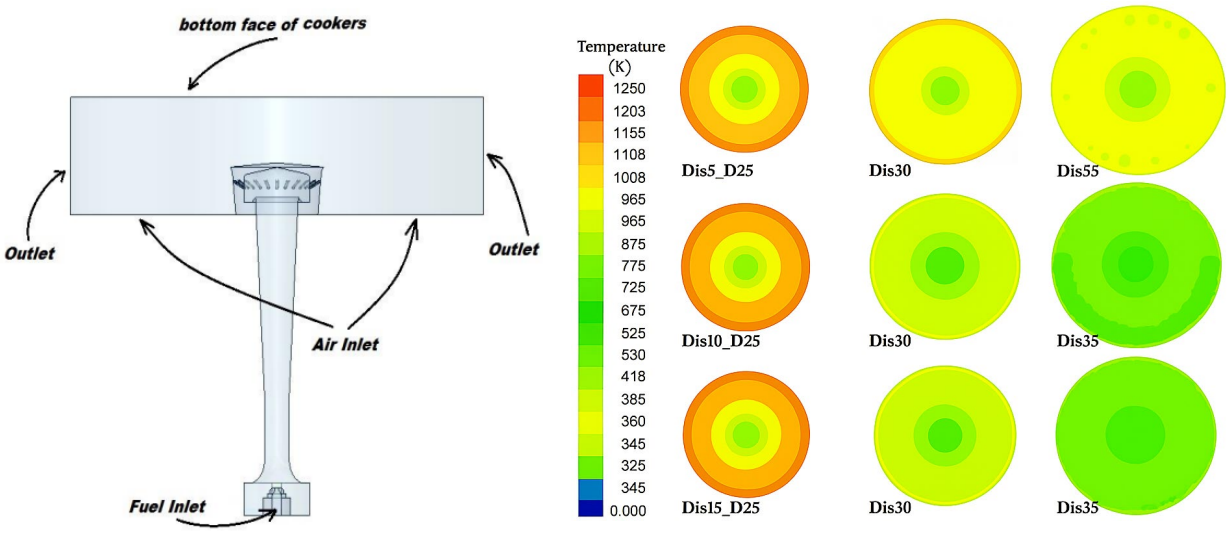

(a) (b)

Figure 8. Sener Burner [30]: (a) 3D model of the burner; (b) Temperature of the burner with variated distance from bottom to head burner (5 cm, 10 cm, 30 cm), and cocker diameter (25 cm, 30 cm, 35 cm).

Subsequently, the combustion phase extended for approximately 8 minutes, characterized by a stable flame exhibiting temperatures in the range of 480 °C to 750 °C, while maintaining a constant fuel mass flow rate of 60 mL·min^{-1}. This phase demonstrated clear flame stability and a distinct jet flame profile. As shown in Figure 7, the flame, which resembled a laminar diffusion flame, initially formed a contracted blue reaction zone extending 10 mm from the burner nozzle. This was followed by a luminous main flame zone rising to approximately 90 mm, and a terminal yellow product zone extending a further 40 mm. The evaluation of combustion gases pointed to trivial emissions, with carbon monoxide (CO) quantified at 0.01 %, carbon dioxide (CO_2) at 0.2 %, and unconsumed hydrocarbons (HC) recorded at 27 ppm. The highest recorded temperature, 750 °C, was observed at thermocouple 3, positioned second closest to the burner nozzle. After the main combustion phase, residual fuel continued to burn independently for an additional 2 minutes until complete flame extinction occurred.

Şener *et al.* [30] conducted a similar experiment to observe temperature of a designed burner, as shown in Figure 8(a). This experiment included two types of variations, the diameter of the holes and the distance between the burner head and the bottom face of the cooker. The variations were aimed at determining the specific conditions required to produce the highest flame temperature.

Based on the results of Şener *et al.* [30], shown in Figure 8(b), the shortest distance from the hole failed to yield the highest temperature. The highest temperature of Seners burner was recorded at a distance of 10 cm, reaching 1008 K or 734 °C [30]. Similarly, in Honai burner experiment, the highest temperature was recorded at thermocouple number 3, located second to the burner, with temperature of 750 °C, as shown in Figure 8. A numerical simulation using computational fluid dynamics (CFD) was carried out on Honai burner to identify the fluid flow patterns and the mixing of fuel and air. This simulation was conducted to compare the results of the experiments, focusing on parameters such as speed, pressure, and temperature. The walls of the combustion chamber are represented as solid boundaries similar to a glass casing, separating the chamber from the surrounding air. The aim was to ensure that the conditions in the combustion chamber were similar to the ones outside.

A replica with dimensions of 110 mm by 45 mm was fabricated to represent the size of the combustion chamber in Honai burner. In the computational analysis, the term remaining bioethanol exhaust gas refers to the pressure-outlet condition necessary to release the exhaust gas flow rate. To simulate direct contact with the surrounding air, the bottom wall of the chamber is designated as velocity inlet with zero airflow. Velocity distribution vector of the enclosed bioethanol fluid is ignored, while the fuel flow rate is set at 60 mL sec-1. This method ensures consistency in fuel speed exiting the burner mouth, allowing the jets to expand to the burst limit in the combustion chamber system. However, the word area signifies the region where the fuel reaction rate and mass fraction remained unchanged due to minimal impact from viscous shear forces and potential-core diffusion. There is no change in the molecular weight of bioethanol gas spray, maintaining consistent density. Figure 9 shows the

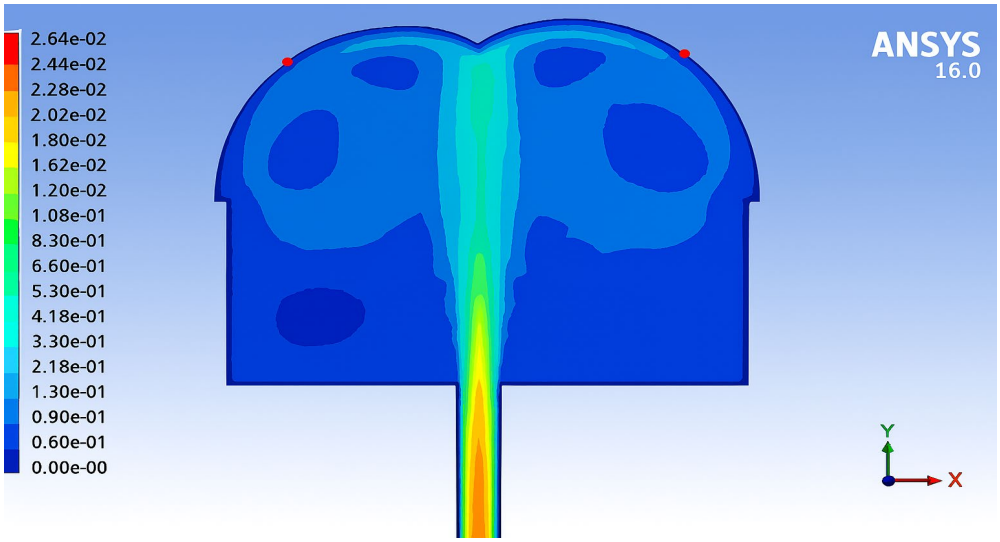

Figure 9. The contour of fuel fusion speed in Honai burner.

results of CFD simulation performed on Honai burner. It shows velocity contours of the fuel wick in Honai burner, with bioethanol fuel diffusing radially outward while the air, acting as the oxidizer, diffuses inward. The reaction zone near flame surface represents the region where bioethanol-oxygen mixture achieves stoichiometric conditions, producing laminar combustion.

IV. Conclusion

The empirical assessment revealed that an 80 % v/v bioethanol derived from sago dregs generated a consistent laminar diffusion flame with a maximum temperature of 756 °C, remarkably low emissions (0.012 % CO, 0.21 % CO_2, and 26 ppm unburned hydrocarbons), and complete combustion at a steady flow rate of 60 mL·min^{-1} utilizing a 14-nozzle Honai burner positioned at a 45° angle. This performance was on par with or in some instances surpassed that of traditional bioethanol fuels. In light of these results, forthcoming investigations should focus on the long-term endurance of the Honai burner during sustained bioethanol use to ascertain material compatibility and seal integrity. Concurrently, an extensive techno-economic analysis is imperative to assess the logistics, production expenses, and scalability of bioethanol derived from sago dregs for domestic applications. Comparative experiments with other lignocellulosic byproducts such as cassava peels or sugarcane bagasse would further clarify relative efficiencies, emission characteristics, and life-cycle ramifications. Moreover, the advancement of hybrid combustion systems integrating adaptive air-fuel regulation or exhaust heat recovery could enhance burner efficacy across diverse environmental and operational scenarios. Thus, sago dregs bioethanol presents considerable promise as an economically viable, low-emission cooking fuel that has the potential to substantially improve sustainable energy accessibility in rural and isolated regions.

Acknowledgements

The authors acknowledge the support of Cenderawasih University, LPPM of Cenderawasih University, and Engineering Faculty of Cenderawasih University.

Declarations

Author contribution

J.J. Numberi, T.K.M. Uniplaita, A. Suwandi, J.P. Siregar, A. Ekayuliana, J. Joni, P. Palamba and M. Liga contributed equally as the main contributor of this paper. All authors read and approved the final paper.

Funding statement

This research did not receive any specific grant from funding agencies in the public, commercial, or not-for-profit sectors.

Competing interest

The authors declare that they have no known competing financial interests or personal relationships that could have appeared to influence the work reported in this paper.

Additional information

References

[1] S. Mujiyanto and G. Tiess, "Secure energy supply in 2025: Indonesia's need for an energy policy strategy," *Energy Policy*, vol. 61, pp. 31–41, Oct. 2013.

[2] A. S. Suntana, K. A. Vogt, E. C. Turnblom, and R. Upadhye, "Bio-methanol potential in Indonesia: Forest biomass as a source of bio-energy that reduces carbon emissions," *Applied Energy*, vol. 86, pp. S215–S221, Nov. 2009.

[3] Y. Yudiartono, J. Windarta, and A. Adiarso, "Sustainable long-term energy supply and demand: The gradual transition to a new and renewable energy system in Indonesia by 2050," *Int. J. Renew. Energy Dev.*, vol. 12, no. 2, pp. 419–429, Mar. 2023.

[4] T. Numjuncharoen, S. Papong, P. Malakul, and T. Mungcharoen, "Life-cycle GHG emissions of cassava-based bioethanol production," *Energy Procedia*, vol. 79, pp. 265–271, Nov. 2015.

[5] S. Papong and P. Malakul, "Life-cycle energy and environmental analysis of bioethanol production from cassava in Thailand," *Bioresource Technology*, vol. 101, no. 1, pp. S112–S118, Jan. 2010.

[6] S. Soeprijanto, L. Qomariyah, A. Hamzah, and S. Altway, "Bioconversion of industrial cassava solid waste (onggok) to bioethanol using a saccharification and fermentation process," *Int. J. Renew. Energy Dev.*, vol. 11, no. 2, pp. 357–363, May 2022.

[7] M. H. S. Ginting, Irvan, E. Misran, and S. Maulina, "Potential of durian, avocado and jackfruit seed as raw material of bioethanol: a review," *IOP Conf. Ser.: Mater. Sci. Eng.*, vol. 801, no. 1, p. 012045, May 2020.

[8] H. Rahman, A. Nehemia, and H. P. Astuti, "Investigating the potential of avocado seeds for bioethanol production: A study on boiled water delignification pretreatment," *Int. J. Renew. Energy Dev.*, vol. 12, no. 4, pp. 648–654, Jul. 2023.

[9] Y. S. Chandrasiri, W. M. L. I. Weerasinghe, D. A. T. Madusanka, and P. M. Manage, "Waste-based second-generation bioethanol: A solution for future energy crisis," *Int. J. Renew. Energy Dev.*, vol. 11, no. 1, pp. 275–285, Feb. 2022.

[10] M. Yasuda, Y. Ishii, and K. Ohta, "Napier grass (Pennisetum purpureum Schumach) as raw material for bioethanol production: Pretreatment, saccharification, and fermentation," *Biotechnol Bioproc E*, vol. 19, no. 6, pp. 943–950, Nov. 2014.

[11] D. S. Awg-Adeni, K. B. Bujang, M. A. Hassan, and S. Abd-Aziz, "Recovery of glucose from residual starch of sago hampas for bioethanol Production," *BioMed Research International*, vol. 2013, pp. 1–8, 2013.

[12] N. A. Bukhari, S. K. Loh, N. Abu Bakar, and M. Ismail, "Hydrolysis of residual starch from sago pith residue and its fermentation to bioethanol," *Sains Malaysiana*, vol. 46, no. 8, pp. 1269–1278, Aug. 2017.

[13] M. Vincent, B. R. Anak Senawi, E. Esut, N. Muhammad Nor, and D. S. Awang Adeni, "Sequential saccharification and simultaneous fermentation (SSSF) of sago hampas for the production of bioethanol," *Sains Malaysiana*, vol. 44, no. 6, pp. 899–904, Jun. 2015.

[14] M. Rijal, "Bioethanol from sago waste fermented by baker's and tapai yeast as a renewable energy source," Jan. 06, 2020, Developmental Biology.

[15] I. M. K. Dhiputra and N. J. Jonatan, "The utilization of metroxylon sago dregs for eco-friendly bioethanol stove in Papua, Indonesia," *KEn*, vol. 2, no. 2, p. 119, Dec. 2015.

[16] B. Susanto et al., "Characterization of sago tree parts from Sentani, Papua, Indonesia for biomass energy utilization," *Heliyon*, vol. 10, no. 1, p. e23993, Jan. 2024.

[17] N. J. Jonatan, A. Ekayuliana, I. M. K. Diputra, and Y. S. Nugroho, "Analysis of the heat release rate of low-concentration bioethanol from sago waste," *International Journal of Technology*, vol. 8, no. 3, p. 428, Apr. 2017.

[18] F. H. Pendi, W.-J. Yan, H. Hussain, H. A. Roslan, and N. Julaihi, "Advances in sago palm research: A comprehensive review of recent findings," *Sains Malaysiana*, vol. 52, no. 11, pp. 3045–3059, Nov. 2023.

[19] D. Waluyo. (2024, Aug. 9). Indonesia.go.id - Lahan Sagu Terluas di Dunia, Peluang Ekonomi dan Ketahanan Pangan Indonesia. [Online] [Accessed: 03-July-2025].

[20] J. Chen, X. Peng, Z. Yang, and J. Cheng, "Characteristics of liquid ethanol diffusion flames from mini tube nozzles," *Combustion and Flame*, vol. 156, no. 2, pp. 460–466, Feb. 2009.

[21] N. Oliverio, A. Stefanopoulou, L. Jiang, and H. Yilmaz, "Ethanol detection in flex-fuel direct injection engines using in-cylinder pressure measurements," *SAE Int. J. Fuels Lubr.*, vol. 2, no. 1, pp. 229–241, Apr. 2009.

[22] S. Yousufuddin, "Combustion duration influence on hydrogen-ethanol dual fueled engine emissions: An experimental analysis," *J. Mechatron. Electr. Power Veh. Technol.*, vol. 9, no. 2, pp. 41–48, Dec. 2018.

[23] W. Widiyanti, M. A. Mizar, C. A. Wicaksana, D. Nurhadi, and K. M. Moses, "Exhaust emissions analysis of gasoline motor fueled with corncob-based bioethanol and RON 90 fuel mixture," *J. Mechatron. Electr. Power Veh. Technol.*, vol. 10, no. 1, pp. 24–28, Dec. 2019.

[24] M. Li, Y. Wang, H. Cheng, Y. Jiang, and C. Zhang, "Influence of nozzle structure on the combustion performance of a graphitic hydrogen-chlorine synthesis combustor," *Applied Thermal Engineering*, vol. 219, p. 119603, Jan. 2023.

[25] Muhaji and D. H. Sutjahjo, "The characteristics of bioethanol fuel made of vegetable raw materials," *IOP Conf. Ser.: Mater. Sci. Eng.*, vol. 296, p. 012019, Jan. 2018.

[26] J. Elias et al., "Thermocouple-based thermometry for laminar sooting flames: Implementation of a fast and simple methodology," *International Journal of Thermal Sciences*, vol. 184, p. 107973, Feb. 2023.

[27] V. Larnaudie, E. Rochón, M. D. Ferrari, and C. Lareo, "Energy evaluation of fuel bioethanol production from sweet sorghum using very high gravity (VHG) conditions," *Renewable Energy*, vol. 88, pp. 280–287, Apr. 2016.

[28] W. Braide, I. Kanu, U. Oranusi, and S. Adeleye, "Production of bioethanol from agricultural waste," *J. Fundam and Appl Sci.*, vol. 8, no. 2, p. 372, May 2016.

[29] R. Mulyawan, R. Nurlaila, T. T. A. R. Ahmadi, M. Muhammad, N. Sylvia, and A. Muarif, "The effects of fermentation extent and acid concentration on bioethanol from HVS paper waste," *Equilibrium Journal of Chemical Engineering*, vol. 7, no. 1, p. 53, May 2023.

[30] R. Şener, M. ÖzdemiR, and M. Yangaz, "Effect of the geometrical parameters in a domestic burner with crescent flame channels for an optimal temperature distribution and thermal efficiency," *Journal of Thermal Engineering*, vol. 5, no. 6, pp. 171–183, Oct. 2019.